Resonance of a Flame in a Parallel-walled Combustion Chamber

by R. A. Dunlap

Approved by E. T. Vincent and R. B. Morrison

UMM-43 March 1950 Project MX 833

(USAF Contract No. W33-038-ac-21100)

engm

UMR0885

ACKNOWLEDGEMENTS

The author wishes to express his appreciation to Mr. R. B. Morrison and Mr. J. Rutkowski for their technical aid and personal encouragement given during the course of this investigation.

LIST OF FIGURES

TABLE OF CONTENTS

LIST OF SYMBOLS

Symbol	Definition
c	Speed of Sound
C	Wave Velocity
l	Length of Column of Unburned Gases
r	Radius of Combustion Sphere or Cylinder
t	Time
L	Length of Combustion Chamber
S	Distance
V_f	Flame Speed, the Rate at which the Flame Front Traverses the Unburned Gas in a Direction Normal to Itself
V_j	Jet Speed of Unburned Combustible Gases
n	Resonant Frequency Cycles/second
ρ_b	Density of Burned Gases
ρ_u	Density of Unburned Gases
v	Volume of Combustion Sphere or Cylinder

SUMMARY

Combustion in a parallel-walled combustion chamber in which all visible burning was completed gave off a definite musical tone. Associated with this tone was a wave motion on the flame front. The observed tone was found to be mainly a function of the position of the flameholder in the combustion chamber and not of flameholder size nor speed of the combustion gases.

Correlation of the frequency of the observed tone with the frequency of tone predicted by assuming resonance of the hot and cold (burned and unburned) gases was found to be good. This correlation indicates that the tone heard and the wave motion on the flame front are the result of resonance. A periodic pulsation of a lower frequency was also observed to be superimposed on the above frequency and was probably due to the Helmholtz type of resonance.

A method is presented for the calculation of flame speeds of this resonant type flame. Predictions of flame speeds by this method agree well with existent data.

INTRODUCTION

The combustor of a propulsion device such as a ram-jet or turbo-jet which burns a mixture of fuel and air in an enclosed space can be idealized as a tube. In the design of this tube-type combustor a number of problems concerned with blowoff, flame stability, ignition limits, pressure and temperature effects of the ambient air, etc., are encountered. In order to better understand these problems a program of theoretical study of the steady flow process, assumed to take place in a combustion chamber, was undertaken (Ref. 1). Experimental verification of the theoretical analysis was attempted through the observation of a V-flame in a parallel-walled, square combustion chamber. A resonant type of combustion was obtained with this equipment. Inasmuch as the flow associated with this resonant burning was unsteady, no information about the characteristics of combustion in a tube could be obtained from a steady flow analysis.

The similarity of combustion in a ram-jet, which is essentially of the closed type, and the burning in a tube, however, lends considerable importance to the resonance phenomena themselves. Rough burning in a ram-jet combustor is a resonance effect and is one of the major problems in ram-jet operation. This rough burning cannot be explained on the basis of knowledge obtained for flames burning in the atmosphere (unconfined).

Previous investigators have reported the resonant condition resulting from combustion in tubes, but no detailed analysis has been found. Research on high speed combustion in tubes as reported in reference 4 indicates that most investigators were interested in the steady flow phenomena associated with combustion and hence modified their tube-type burners so that resonance was not a predominant factor. Such modification usually consisted of moving the flameholder downstream so that the major portion of the burning occurred outside the combustion chamber. The characteristics of this combustion then became similar to those of flames burning in the atmosphere (unconfined); hence these results would not be applicable to ram-jet combustor design.

This paper is a description and a partial analysis of resonant combustion as observed in a small-scale, parallel-walled combustion chamber. It is believed that the results of this analysis may assist in understanding such problems as the "rough burning" phenomena.

The experimental work in this study was carried out in a parallel-walled tube of a one-inch square cross-section in which mixture velocities were varied from 10 to 60 feet per second. Several size flameholders were employed. The fuel used was commercial propane.

This investigation is part of a program of research conducted at the Aeronautical Research Center of the University of Michigan for the United States Army Air Force under contract W33-038 ac 21100 during the year 1949.

DESCRIPTION OF APPARATUS

I. Burner Equipment

The burner equipment used in experimentation with the confined V-flame consisted of commercial rotameters used to measure flow of the air and fuel, a mixing chamber, a plenum chamber with turbulence screens, a nozzle, and a 1" x 1" x 12" square cross-section combustion chamber. A schematic diagram of the equipment is shown in figure 1; a photograph of the equipment is shown in figure 2. Air was obtained from a high pressure (150 psi) lab source; the fuel used for all testing was commercial propane.[1]

The contour of the square nozzle was designed to fit a segment of the Spiral of Archemedes. This design decreased the abruptness of discontinuities in the radius of curvature of the nozzle contour and hence minimized the flow separation which occurred with a nozzle of circular contour. The nozzle as shown in figure 3 had a contraction ratio of 49. A velocity profile of the air stream at the combustion chamber exit was obtained by making a traverse of the stream with a pitot tube .065" in diameter. The profile, shown in figure 4, shows some boundary layer build-up but was considered to be satisfactory for the experimentation summarized in this report.

The combustion chamber consisted of two 1" x 3/4" x 12" solid steel walls and two 1/8" x 3" x 12" Vycor glass plates. The Vycor glass[2] will withstand the large temperature gradient in the combustion chamber whereas pyrex or other types of glass will not. The glass walls were held to the solid walls by means of stainless steel clips, illustrated in the photograph in figure 5. Burning was initiated by means of a spark from a high voltage coil.

II. Flameholders

Several different types and sizes of flameholders were used in the experimentation. The single rod flameholder shown in figure 6a was employed whenever a clearly defined flame front was desired. These rods were centered

[1]Commercial propane sold by the Flamegas Corporation, Detroit, Michigan.

[2]Vycor glass, manufactured by Corning Glass Works, contains 98% $Si\,O_2$. At the present, the cost of Vycor is approximately 1/5 that of quartz.

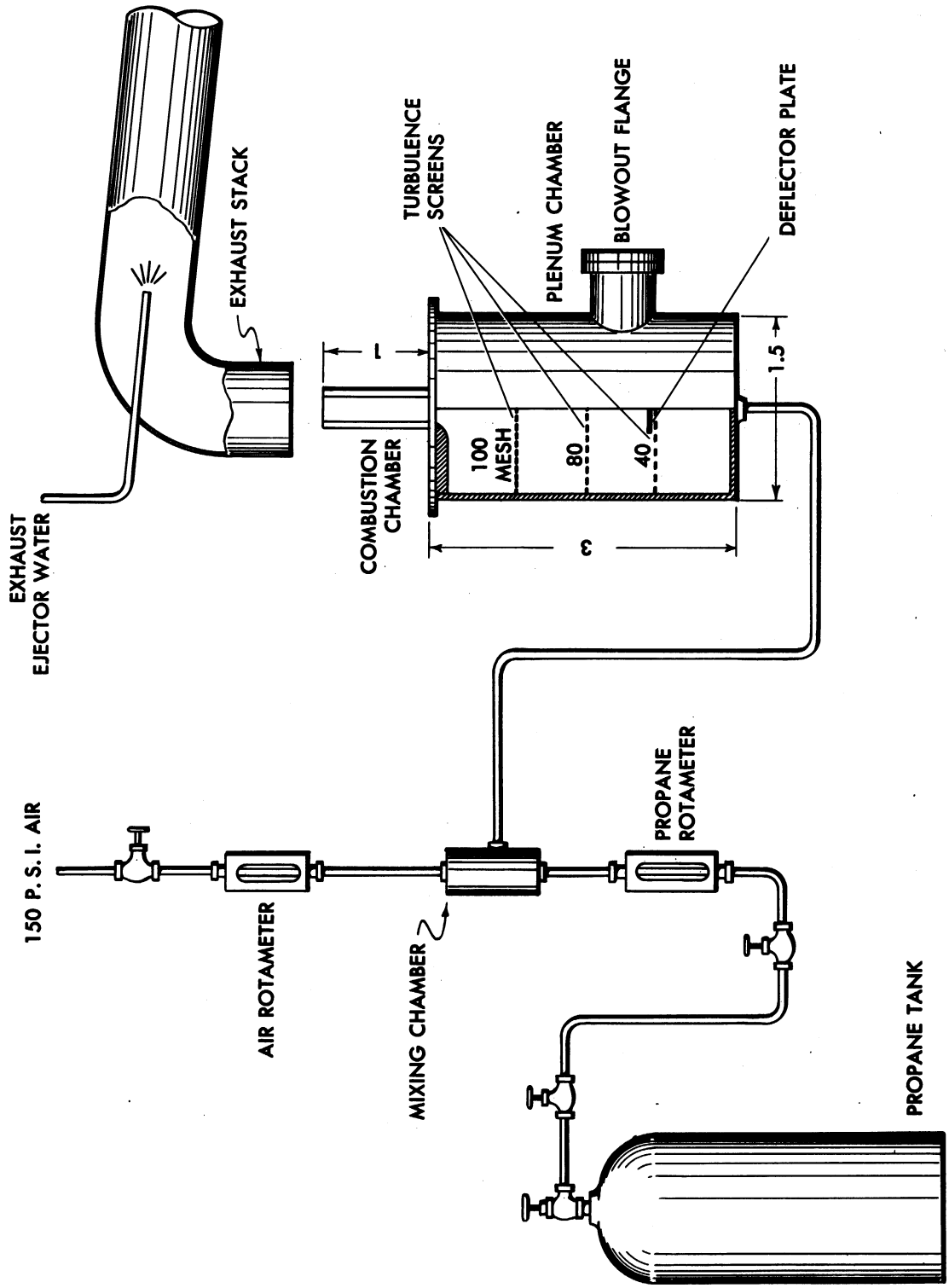

FIG. 1 SCHEMATIC DIAGRAM OF BURNER EQUIPMENT

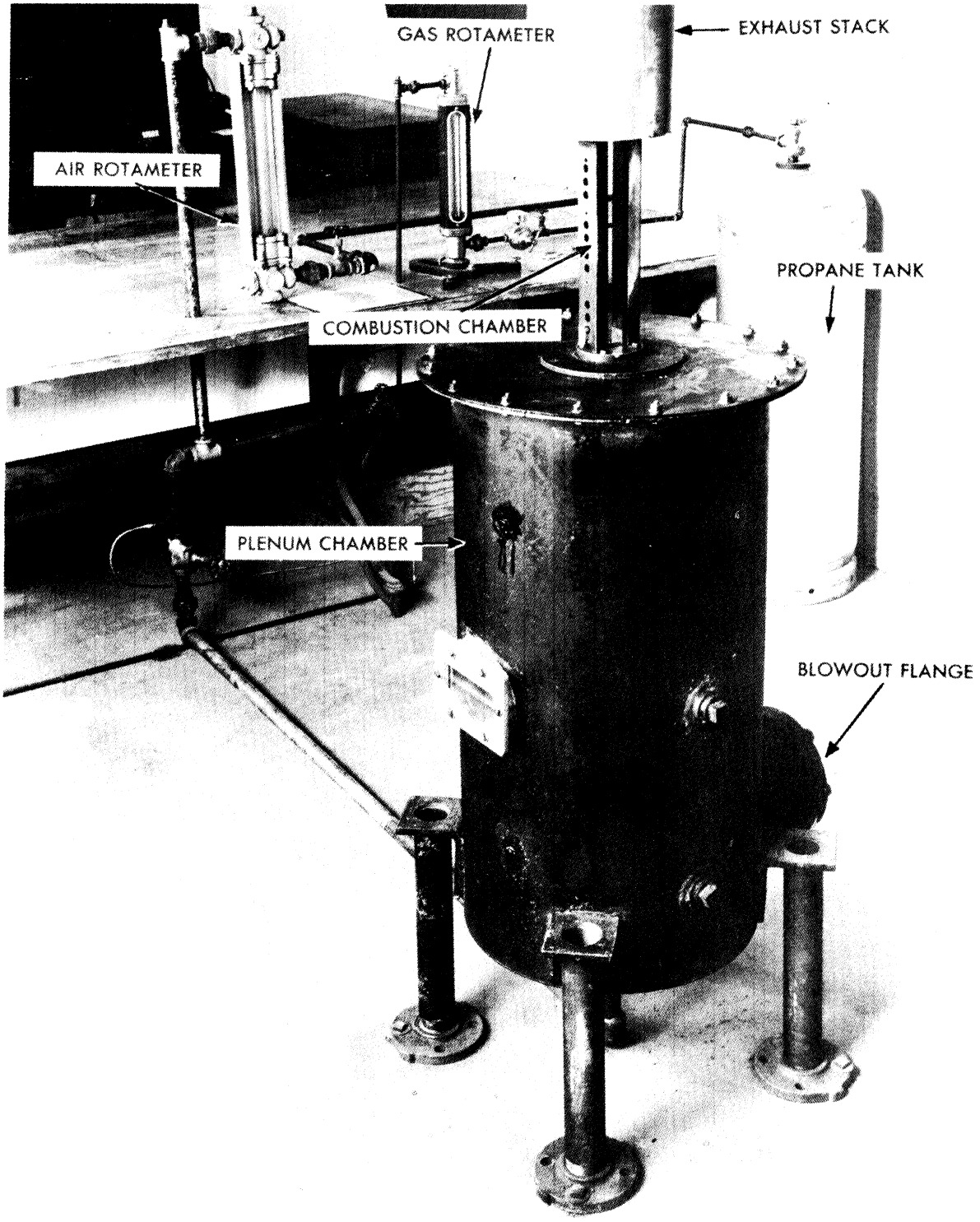

FIG. 2 PHOTOGRAPH OF BURNER EQUIPMENT

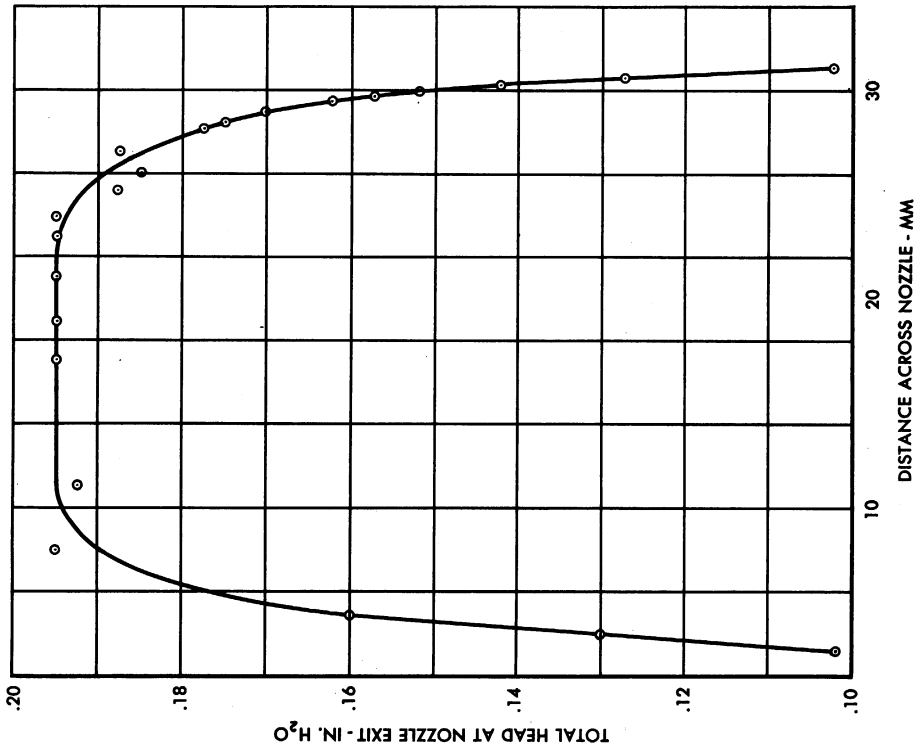

FIG. 4 TOTAL PRESSURE DISTRIBUTION AT COMBUSTION CHAMBER EXIT

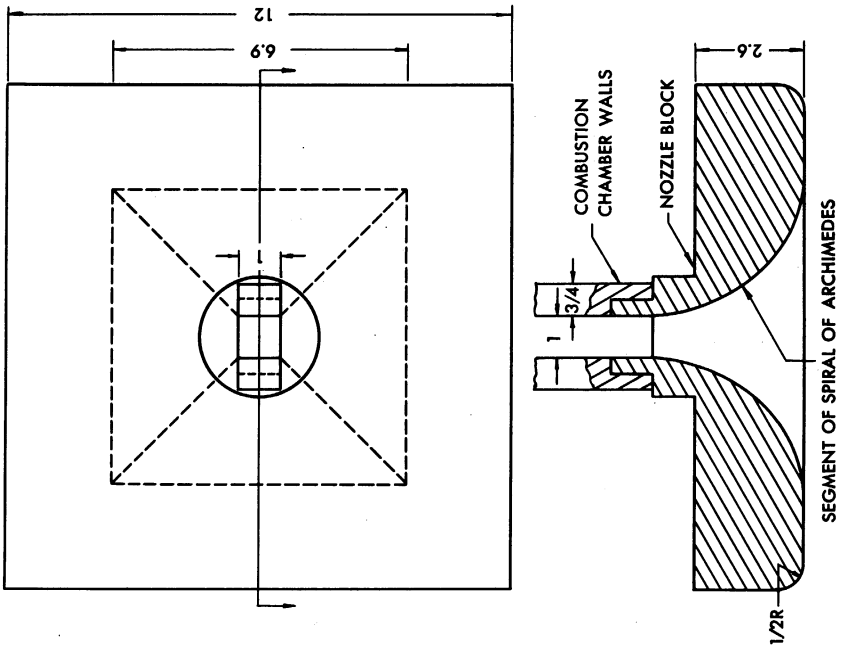

FIG. 3 SKETCH OF SQUARE NOZZLE

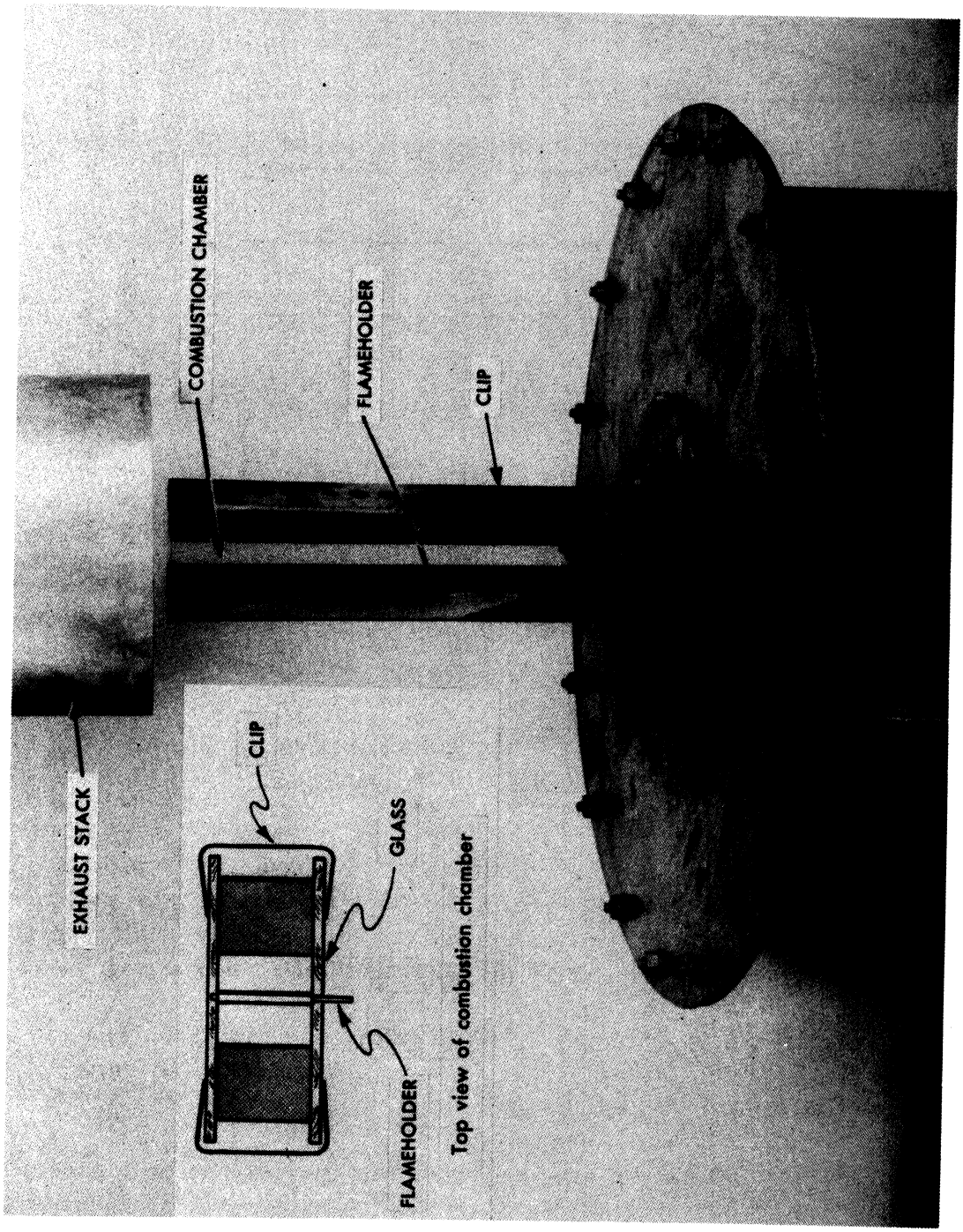

FIG. 5 PHOTOGRAPH OF COMBUSTION CHAMBER

Showing the clips used to hold the glass in place and the method of positioning the flameholder

in the combustion chamber and located at various positions along the chamber axis. The position of the flameholder was fixed by drilling one hole partially through one plate of the Vycor glass and another hole completely through the other plate, as shown in figure 5.

A second type flameholder used is that shown in figure 6b. Because of the multiplicity of holes, a number of small flames will burn from this flameholder, hence allowing the burning to be completed a short distance downstream of the flameholder. This flameholder was held in place in the combustion chamber by friction between the chamber walls and faces c and c'.

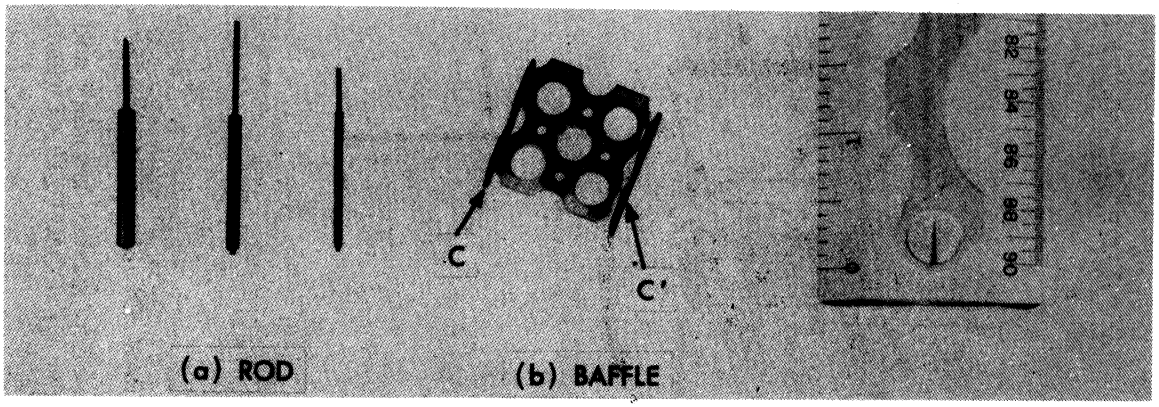

FIG. 6 PHOTOGRAPH OF FLAME HOLDERS

III. Shadowgraph Equipment

A shadowgraph system of simple construction but capable of yielding results of high quality is shown in figure 7. This equipment consisted of a spark source[1] (an approximate 5 microsecond flash in a Liebessart type spark gap) and a shutter. The shutter was synchronized with the spark source and was actuated manually. The speed of the shutter was governed by the spring arrangement shown in figure 7. It was necessary that the speed of the shutter be sufficiently great so that the shadowgraph was not masked by fogging of the film from the light of the flame.

The imperfections in the Vycor glass used for the combustion chamber walls cause the reproduction of all shadowgraphs to have a speckled and wavy appearance. Figure 9 is a shadowgraph of the combustion chamber with no air flowing through it. From this figure it is apparent that a speckled and wavy appearance is not the result of the combustion or flow process.

[1]See Appendix 3 for a schematic diagram of the spark source.

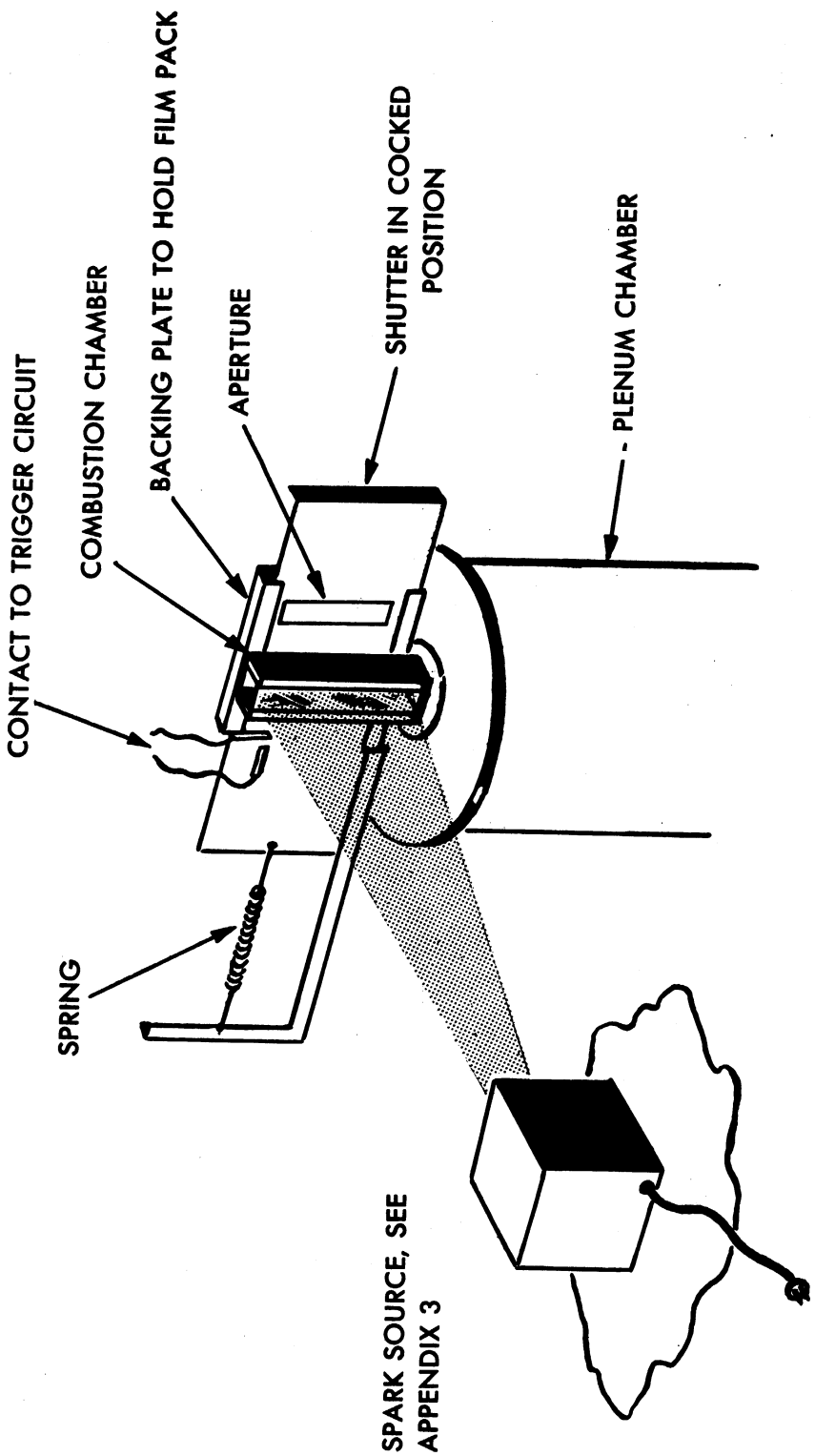

FIG. 7 SCHEMATIC DIAGRAM OF SHADOWGRAPH ASSEMBLY
Showing relative position of combustion chamber and shutter

The distance from the flame to the photographic plate determines the width of the bright band of light (displaced light caused by the density change at the flame front). The shadowgraphs in figure 10 and figure 11 were taken at 12" and 2" respectively. A comparison of these two figures shows that the shadowgraph taken with the photographic plate nearest the flame (Figure 11) is most clearly defined.

The non-parallel appearance of the combustion chamber walls, as seen in figure 10, is the result of the shadowgraph method of photography and is not a physical fact. The temperature gradient along the chamber walls causes a greater refraction of light in the upper (hotter) region. It is noted that this effect is not as apparent in the photograph in figure 11, which was taken with the film plate closer to the flame than it was in figure 10. The effect is not evident at all in figure 9 which is a shadowgraph for the case in which no burning takes place.

Kodak "Contrast Process Panchromatic" film was used for all shadowgraphs.

Shadowgraphs were also taken with a Fastax movie camera at the maximum rate of 5040 frames per second. A sequence of these shadowgraphs is shown in figure 11. The light source used for these shadowgraphs was a continuous operating carbon arc lamp. The shadowgraph of the flame was cast on a ground glass screen; the screen was photographed with the Fastax camera. A schematic diagram of the equipment is shown in figure 8.

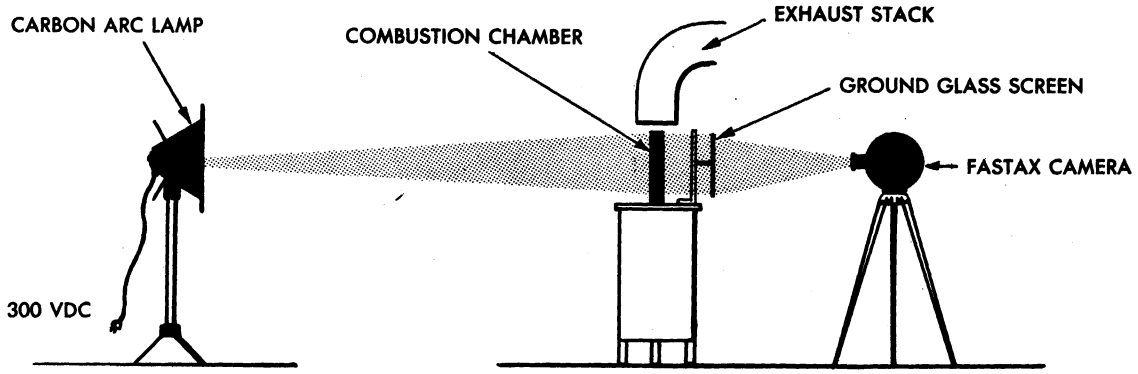

FIG. 8 SCHEMATIC DIAGRAM OF FASTAX SHADOWGRAPH ASSEMBLY

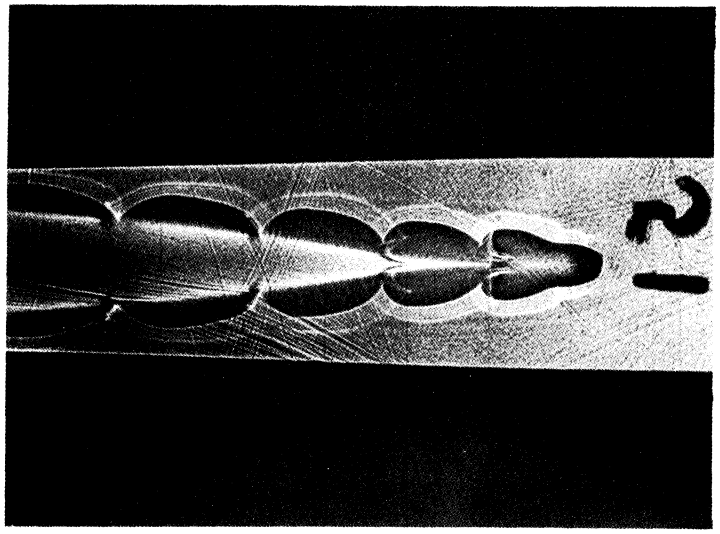

FIG. 10 SHADOWGRAPH OF V-FLAME IN COMBUSTION CHAMBER. RUN No. 51
Film plate 12" from combustion chamber.
Rod flame holder .125" dia. V_j=15 ft. sec.

FIG. 9 SHADOWGRAPH OF COMBUSTION CHAMBER. NO FLOW CONDITION. RUN No. 39

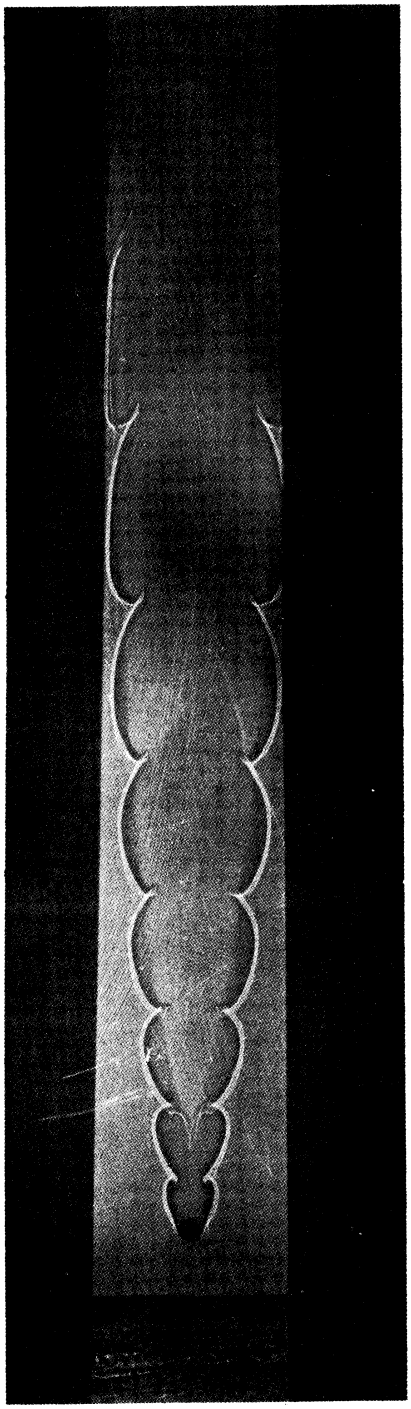

FIG. 11 SHADOWGRAPH OF V-FLAME IN COMBUSTION CHAMBER BURNING FROM A ROD TYPE FLAME HOLDER
Run No. 58 F/A = .063, V_j = 15 ft./sec.

RESULTS AND DISCUSSION

I. Description of Flame

A flame burning from a flameholder in a rectangular, parallel-walled combustion chamber is defined here as a "confined V-flame". The flame is termed "confined" only when all the visible burning takes place within the combustion chamber. This type flame is distinguished from the unconfined V-flame, which is one that burns in the atmosphere. Typical photographs of the confined and unconfined flames are shown in figures 12 and 13, respectively.

Inherent to the confined type flame is the musical tone emitted from the combustion chamber and its different appearance from the unconfined flame. A comparison of the photographs in figures 12 and 13 brings out the difference in the apparent width of the flame fronts. The small insert shown in these figures depicts the cross-section of the flame as it appears to the eye. Shadowgraphs (Figures 11 and 15) of the confined and unconfined two-dimensional flames show that the apparent increase in width of the flame front of the confined flame is due to the flame front assuming a wave shape, the increased width being the envelope of the wave as it moves downstream. Fastax shadowgraphs of this burning were taken at a shutter speed of 5,040 frames per second. A sequence of these shadowgraphs is shown in figure 16 and shows the wave moving toward the chamber exit.

An unconfined, two-dimensional V-flame was obtained by removing the metal walls of the combustion chamber but retaining the glass walls. A photograph of this flame, shown in figure 14, appears to have the same width flame front as the confined flame of figure 12. However, the cross-section of the flame as sketched below the photograph shows that the apparent width of flame front is due to a folding of the flame on the glass walls. A shadowgraph of this same flame (Figure 15) shows that the wave motion on the confined flame front (Figure 11) is not evident, indicating that the glass walls do not affect the wave motion and that complete confinement is necessary for the wave motion and resonant condition.

The effect of jet speed of the combustible mixture on the wave length of the wave is seen from a comparison of figures 17a, 17b, and 17c. From these figures it is apparent that an increase in jet speed caused an increase

Typical cross-section of flame

FIG. 12 PHOTOGRAPH OF CONFINED V - FLAME BURNING FROM A ROD FLAME HOLDER. RUN No. 35

Typical cross-section of flame

FIG. 13 PHOTOGRAPH OF UNCONFINED V-FLAME BURNING FROM A ROD ELAME HOLDER. RUN No. 189

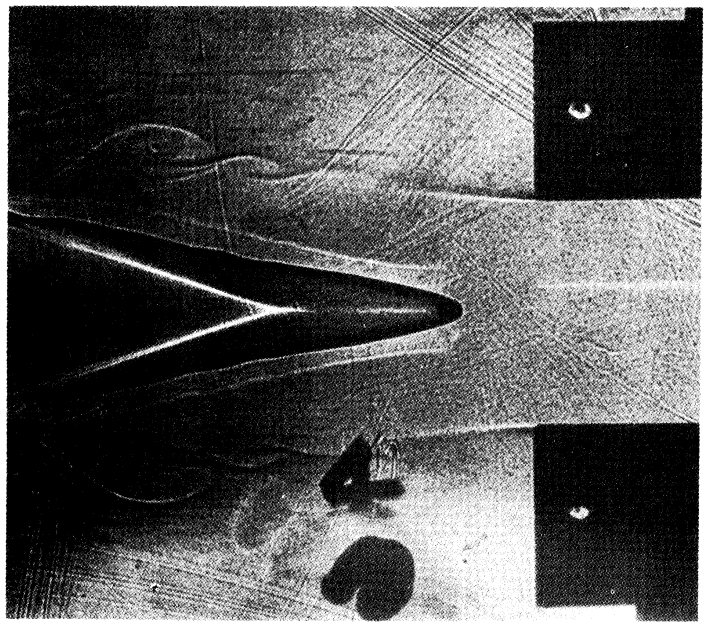

Typical cross-section of flame

FIG. 15 SHADOWGRAPH OF UNCONFINED TWO-DIMENSIONAL FLAME

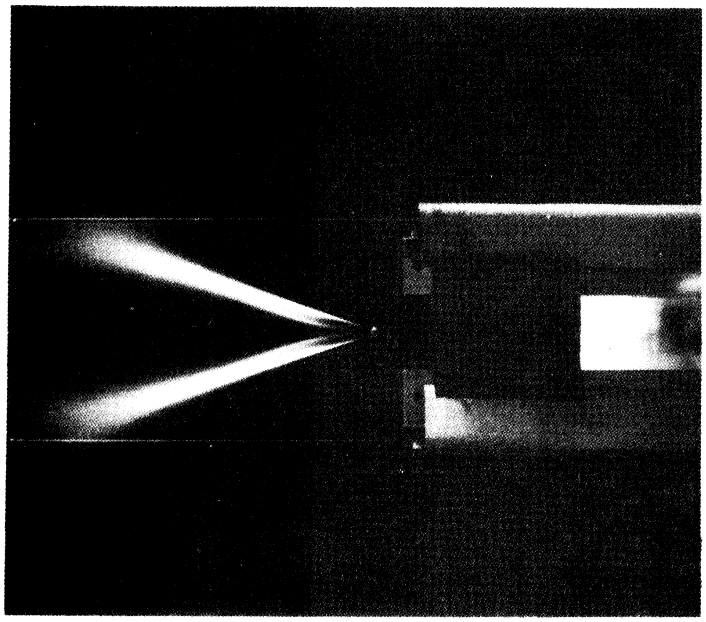

Typical cross-section of flame

FIG. 14 PHOTOGRAPH OF UNCONFINED TWO-DIMENSIONAL FLAME

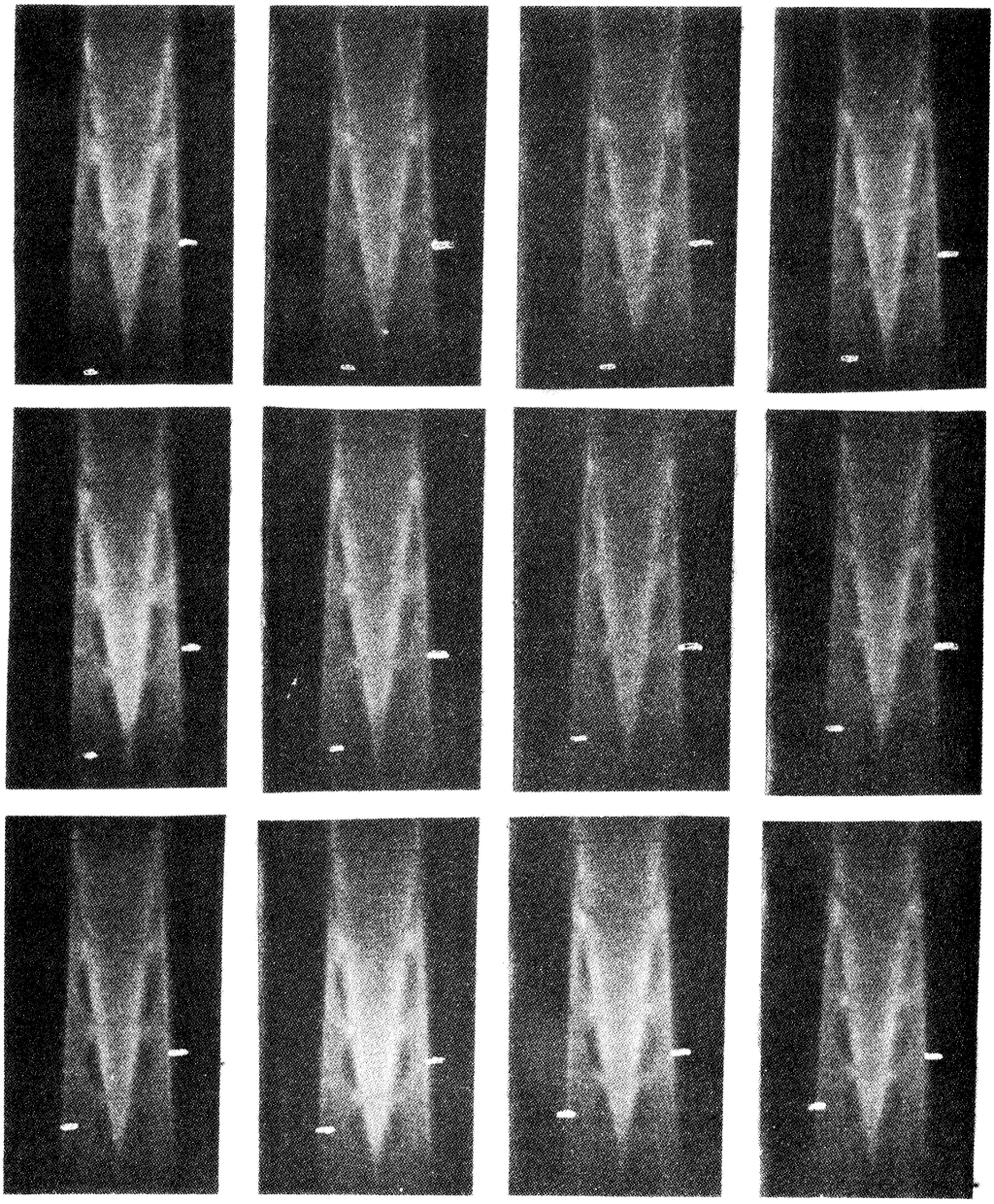

FIG. 16 FASTAX SHADOWGRAPHS OF CONFINED V-FLAMES. No. 1 TO 12

Fastex shadowgraphs of a V-flame in a 1" x 1" rectangular combustion chamber Run #37; V_j = 14 ft/sec; Flameholder .125 dia.; Film speed: 5040 frames/sec.

Progression in time is obtained by reading from left to right and down. The white mark on the right side of the chamber is a reference mark stationary with respect to chamber walls. The mark on the left side follows a wave as the wave progresses from the bottom to the top of the combustion chamber.

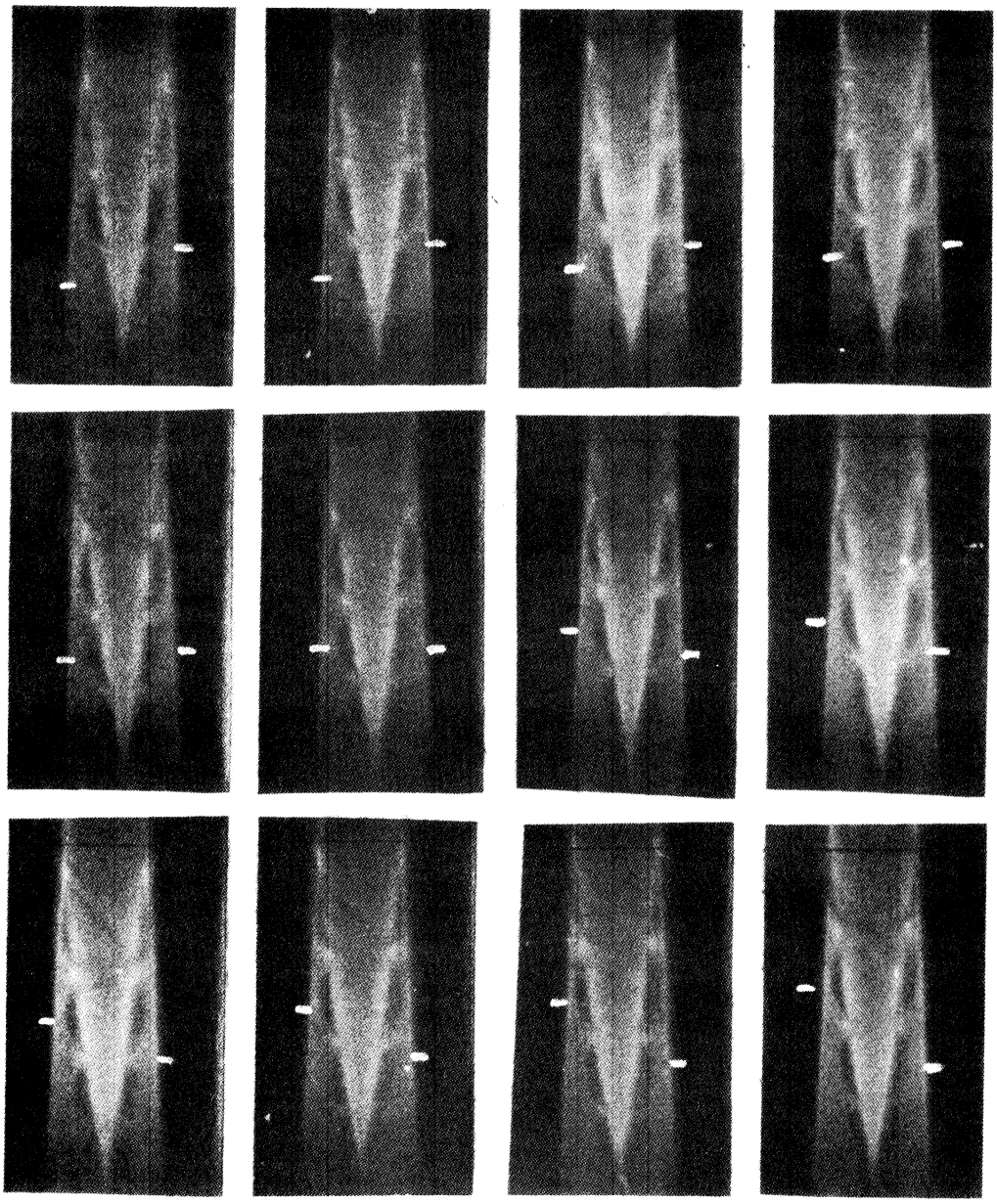

FIG. 16 (CONTINUED) No. 13 TO 24

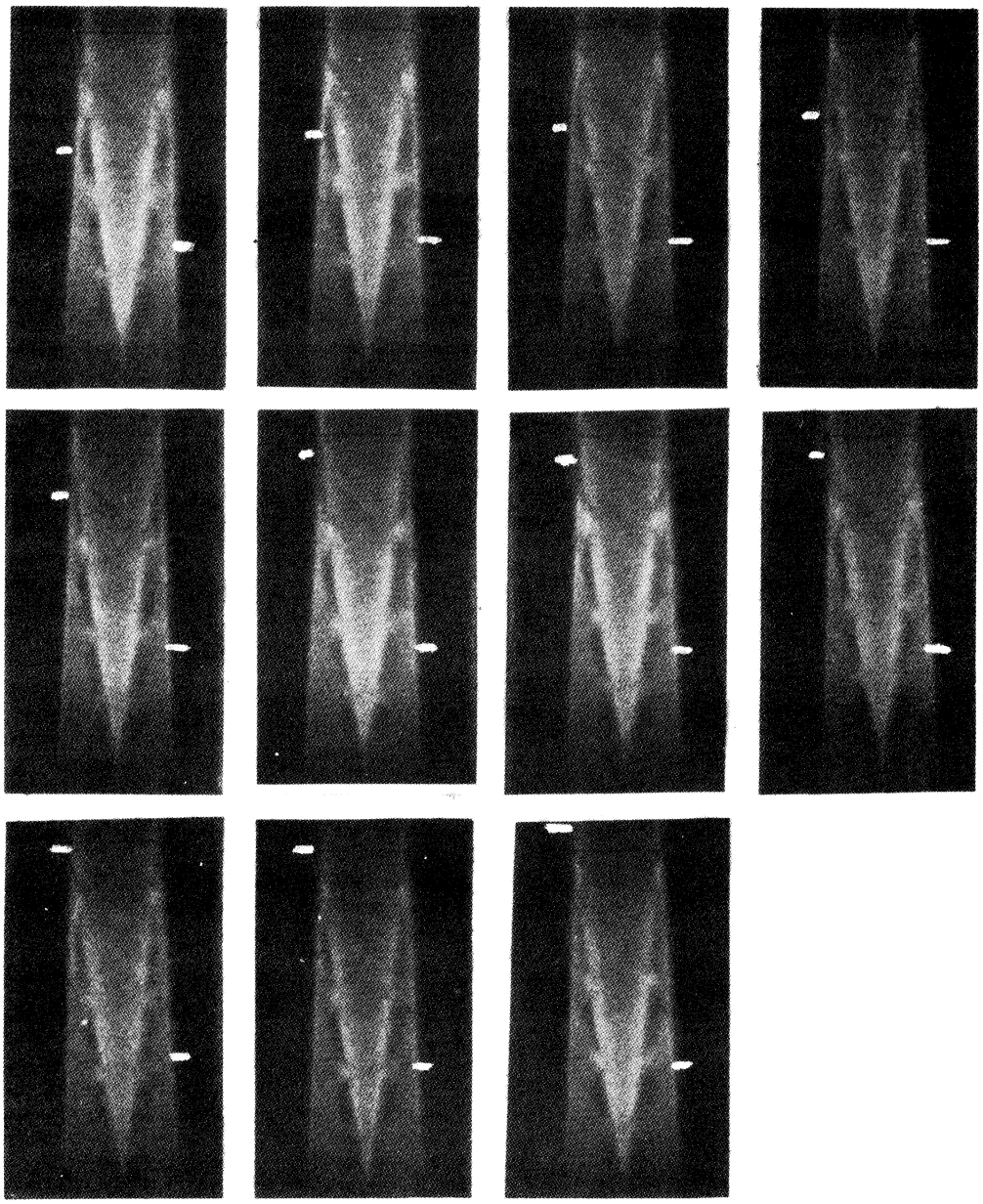

FIG. 16 (CONTINUED) No. 25 TO 35

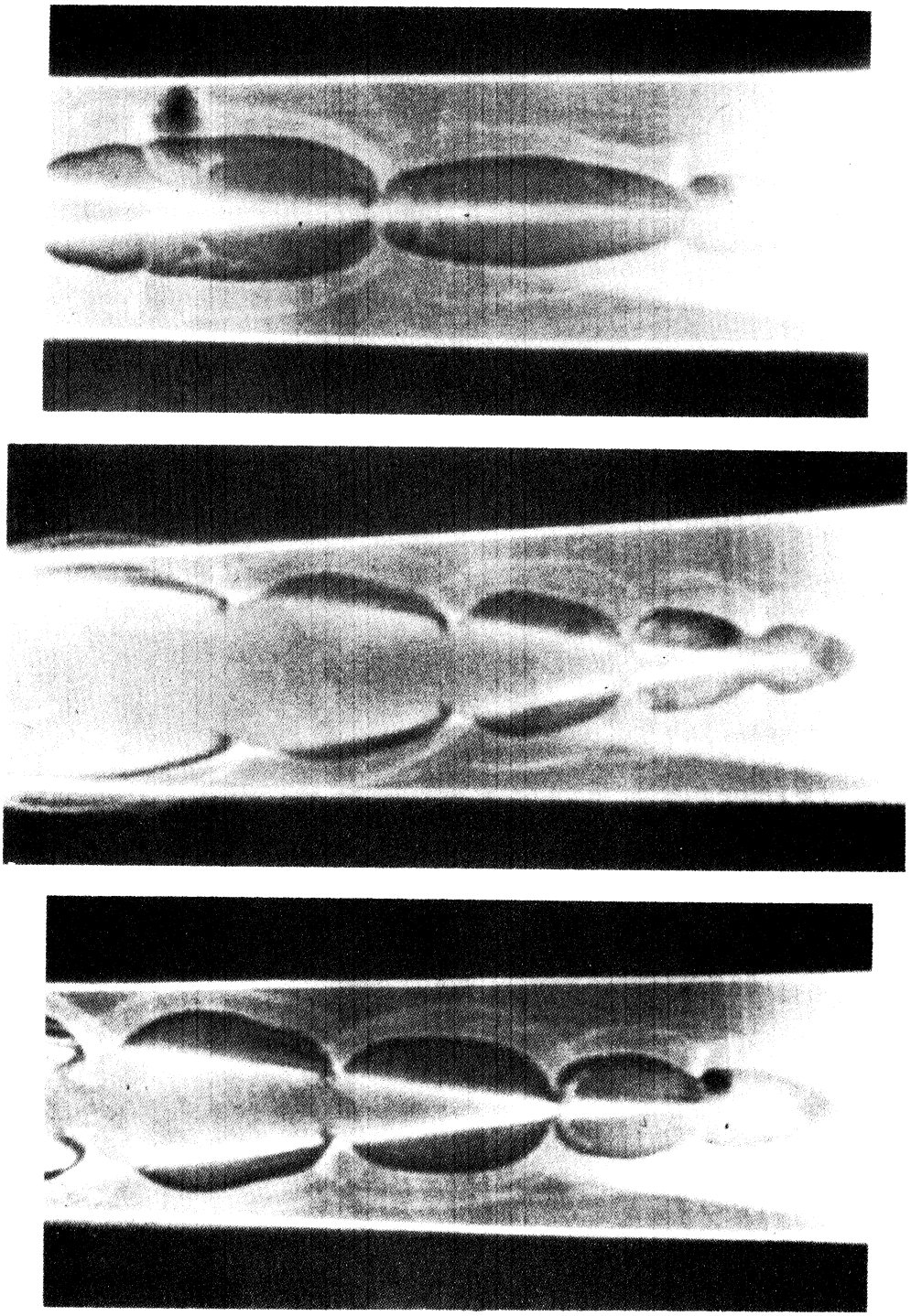

Run No. 21. V_j= 21 ft./sec. Run No. 19. V_j=14.5 ft./sec. Run No. 24. V_j= 33 ft./sec.

FIG. 17 SHADOWGRAPHS OF V-FLAME AT VARIOUS JET SPEEDS—STOICHIOMETRIC F/A RATIO

in wave length. Jet speed was found to have little effect on the frequency of the tone.

II. Cause of Tone and Wave-shaped Flame

It was thought that the tone observed to be emitted from the combustion chamber was that due to resonance of the complex hot (burned) and cold (unburned) gases in the chamber. This type of resonance can be handled very easily mathematically. An expression for the fundamental resonant frequency of a column composed of two gases was derived by solving the one-dimensional wave equation for fixed boundary conditions. The derivation, given in Appendix 1, yields the expression in equation (1) in which the resonant frequency "n" is given in terms of "l" the length of the column of unburned gas.

$$\tan \frac{2\pi n l}{c_1} = -\frac{c_1}{c_2} \tan \frac{2\pi n (L-l)}{c_2} \qquad (1)$$

where

n = resonant frequency cycles per second

L = length of combustion chamber - feet

l = length of column of unburned (cold) gases - feet, equivalent to distance from combustion chamber entrance to flameholder

c_1 = speed of sound in unburned gases - feet per second

c_2 = speed of sound in burned gases - feet per second

A plot of this function is shown in figure 18. On the basis of data for propane-air flames in reference 9, the temperature of the hot gases was assumed, for this plot, to be equal to 2600°R, hence $c_2 = \sqrt{\frac{2600}{520}}\, c_1$.

The flameholder shown in figure 6b was placed in the combustion chamber and its position varied, effectively varying "l" in equation (1). The resulting frequency "n" was noted.[1] In the range of "l" from .5 feet to 1.0 feet the tone became less intense, and hence the frequency could not be determined accurately. A possible reason for the decrease in intensity is that the majority of burning no longer occurred in the chamber, thus changing the resonating conditions. In the range of "l" from 0 to .2 feet the normal tone usually heard was masked by a lower frequency noise which accompanied a large-scale fluctuation of the flame about the flameholder. This large-scale fluctuation usually led to flash back. For these reasons the frequency could not be determined in this range of "l".

Figure 18 is a plot of the fundamental theoretical resonant frequency with the experimental frequencies superposed. As evident from this figure, there is excellent agreement in the region of "l" in which the tone was most distinct (.2 feet < l < .5 feet).[2] This agreement indicates that the tone observed from the combustion chamber is that due to resonance of the hot and cold gas mixture.

It is not known whether the wave moving down the flame front is the cause of or the result of the oscillation in the gaseous mixture. By introducing a perturbation at the flame front, Landau (Ref. 11) shows mathematically that a disturbance at the flame front will continue to grow with time and hence is unstable. It is possible that the wave motion previously described in this report is an example of this type of instability. In this case, however, the amplitude of disturbance does not grow indefinitely but approaches a constant value, that value being the height of the wave crest (Figure 11).

[1]The frequency of the tone caused by burning was obtained by audibly matching this tone with the tone produced by an audio oscillator. When the beat note disappeared, the two frequencies were matched. This was found to be reproducible to within 20 cps. The results obtained by this method were checked with calculations of the wave frequency obtained from the Fastax shadowgraph movies. The two frequencies checked to within 40 cps.

[2]It should be noted that equation (1) was developed by assuming a surface of discontinuity between the hot-cold gases which was normal to the direction of flow. Burning which occurred from the flameholder previously mentioned was completed in a very short distance, and hence the conditions of equation (1) are closely approximated. The flame surface resulting from burning from the rod type flameholder shown in figure 4a forms a wedge (Fig. 12) and hence does not satisfy the conditions in equation (1). For a given location of the flameholder in the combustion chamber there was observed to be a 170 cps difference in tone emitted from the chamber for the rod and baffle type flameholder.

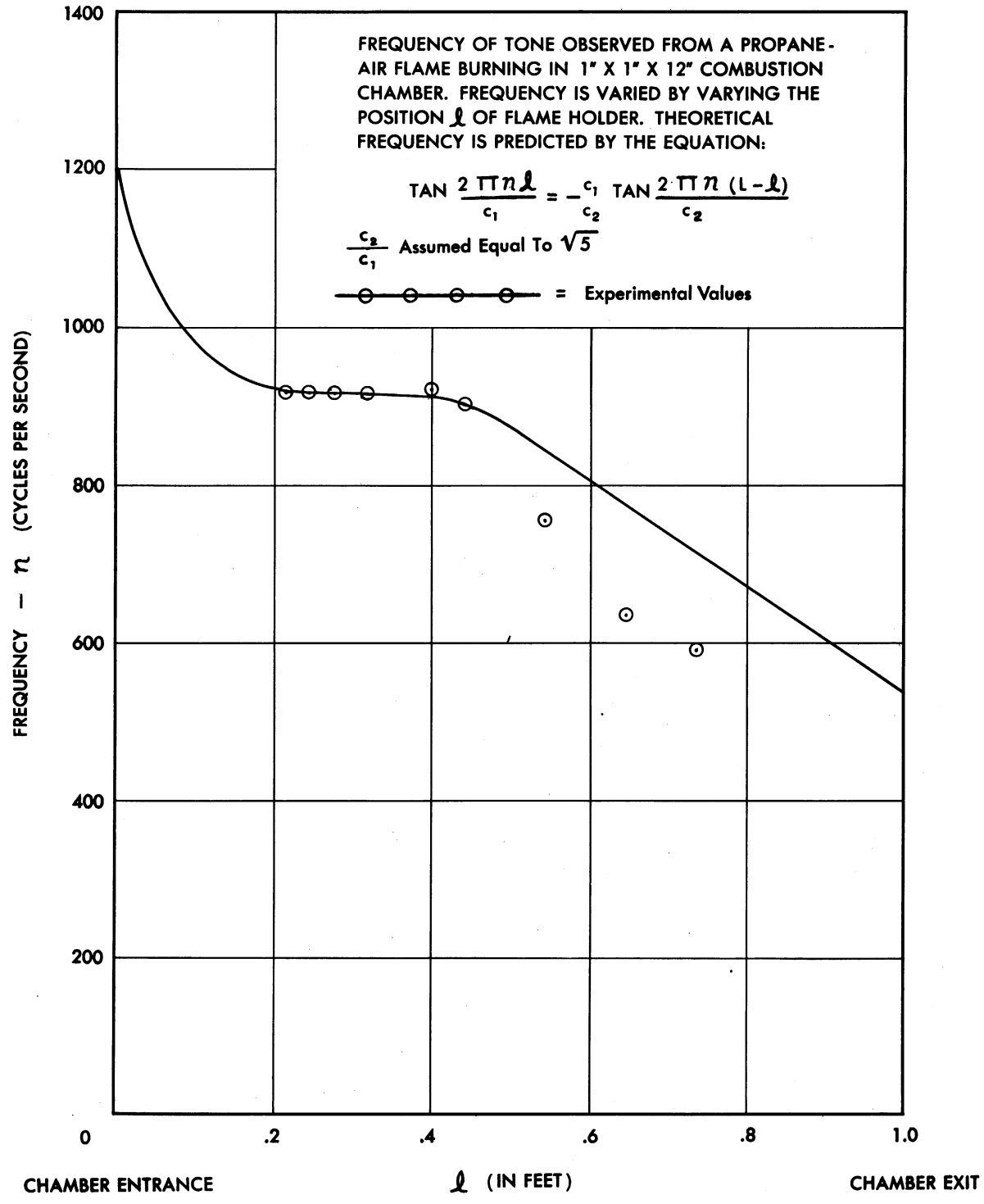

FIG. 18 PLOT OF n vs ℓ

III. The Low Frequency Fluctuation

The flame began a low frequency, large-scale oscillation about the flameholder when the flameholder was placed near the combustion chamber entrance ($0 < l < .2$). The frequencies of this oscillation were observed to be between 5 and 20 cps. Calculations for the frequency of a Helmholtz resonator for the system involved yield frequencies close to those observed, indicating that this low frequency tone is probably due to the Helmholtz type resonation.

IV. Method for Calculating Flame Speeds of Confined V-flame

A primary reason for research on the confined V-flame was to find a method for determining characteristics of the confined flame, such as flame speed, velocity gradients, and so forth. By a Huygens wave analysis of the confined flame it was found possible to compute flame speeds of the resonant V-flame. An analysis of this type for an unconfined V-flame is found in reference 9.

Flame speed is here defined as the rate at which a flame front enters the unburned gas, relative to the unburned gas and normal to the unburned gas. Consider an ignition center, as in figure 19a, moving through a stagnant combustible mixture, igniting it at definite time intervals at points A, B, C, D, and so forth. The combustion zone for a point ignition source will be a sphere, and for a line ignition source, a cylinder.

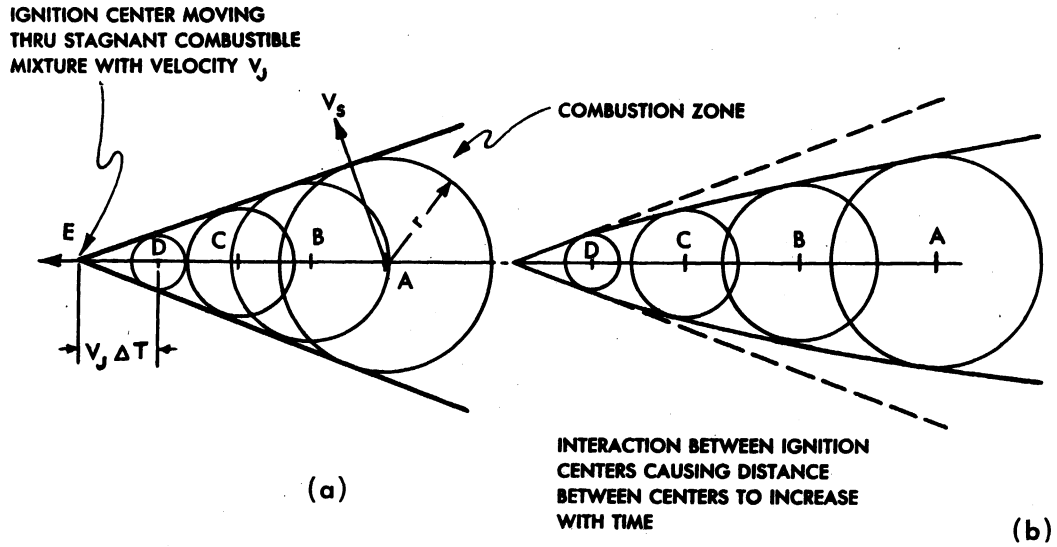

FIG. 19 IGNITION CENTER MOVING THROUGH COMBUSTIBLE GAS

If there were no interaction[1] between ignition centers, then as the time interval decreased to zero, the envelope of the combustion zones would be a cone for a three-dimensional axi-symmetrical flame, or an isoceles wedge for a two-dimensional flame. If there were interaction between centers the flame front would no longer be straight and the envelope would be such as shown in figure 19b. In either case, the flame front moves outward from the ignition centers with a spatial velocity $V_s = \frac{dr}{dt}$. Assume now that the flame is two-dimensional, i.e., ignition takes place along a line, so that the flame propagates from the centers A, B, etc., as a cylinder.

Then:

Area of cylinder = $2 \pi r \times 1$

Volume = $\pi r^2 \times 1$

Volume increase due to burning = $\frac{\rho_u}{\rho_b} V_f \, 2 \pi r \, dt$

$dv = 2 \pi r \, dr$

so $2 \pi r \, dr = V_f \, 2 \pi r \, dt \frac{\rho_u}{\rho_b}$

so $\frac{dr}{dt} = V_f \frac{\rho_u}{\rho_b}$

or $V_f = \frac{\rho_b}{\rho_u} \frac{dr}{dt}$

Between ignition centers A and B, for example, the average flame speed will then be given by $V_f = \frac{\Delta r}{\Delta t} \frac{\rho_b}{\rho_u}$ (2)

The confined type flame observed in the combustion chamber lends itself nicely to flame speed calculations of this type.

[1]By interaction is meant a relative movement between the centers, caused perhaps by unequal forces upon expansion of the spheres at each ignition center.

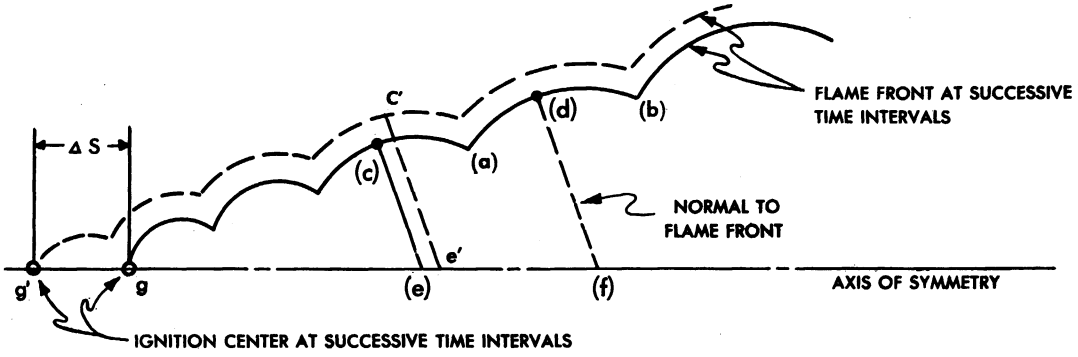

FIG. 20 PROFILE OF CONFINED FLAME AT SUCCESSIVE TIME INTERVALS

Consider first the flame front shown as a solid line in figure 20. If this flame were stationary with respect to the burner walls (combustible gases moving) then the time required for the wave crest at (a) to move to (b), or some point (c) to move to (d), is just the period of the wave motion $\frac{1}{n}$. If now the ignition center (e.g. (A) in figure 19) moved with the same velocity as the wave velocity, then this time interval ($\frac{1}{n}$) would be the same as the time required for the radius at c (Figure 20) to grow from c-e to d-f. A criterion for determining whether the ignition centers moved with the wave velocity is as follows: allow the ignition center (g) in figure 20 to move forward a distance $\Delta s = V_j \Delta t$ (reference the unburned gas) to point (g'). The flame front will now have the shape shown in dashed lines due to expansion of spheres in time Δt. If the particle at point (c) on the flame front now moves with the same relative velocity as the wave, the flame front would maintain its shape and a normal to the flame front at (c) would be nearly parallel[1] to the normal to the flame at (c'). The difference between the lengths of the normals would then be $\Delta r = c'e' - ce$. Since $V_f = \frac{\Delta r}{\Delta t} \frac{\rho_b}{\rho_u} = n\Delta r \frac{\rho_b}{\rho_u}$ and n, Δr and $\frac{\rho_b}{\rho_u}$ are all available quantities, the flame speed is determinate.

Average flame speeds along the flame front were calculated between points where the normals to the flame surface were approximately parallel. These calculations are presented in Appendix 2. The density ratio data, obtained from previous research, are found in reference 9. Within the accuracy of the calculations, it was found that flame speeds calculated in this manner agree very well with flame speeds for the confined V-flame as calculated by other observers (Ref. 4, p. 26).

[1]The normals would be exactly parallel if the flame front were straight. Due to confinement, the front has a slight curvature.

V. Other Observations

In the course of this investigation a number of interesting effects have been noted. Some of the observations which have not been previously discussed are mentioned below.

1. At one time it was thought possible that the wave on the flame front was the result of vortices of the Karman vortex type shedding from the flameholder. Since the frequency at which this type of vortex is shed is dependent on the body diameter (in this case a cylinder), the diameter of flameholders was varied and the resulting tone noted. It was found that flameholder diameter had no effect on the tone observed. Hence it is concluded that the resonance condition is not a result of a vortex motion at the flame front.

2. A streamline of Ti Cl_4 vapor was put into the flow field for visual observation. The photograph in figure 22 shows that the streamline in the burned gases does not become diffuse, indicating that no large scale turbulence was caused by the wave or the burning process.

3. A secondary flameholder was placed downstream of the rod flameholder (Figure 21). When the distance "y" between the first and second flameholders reached a critical value, the flame began to burn very violently and noisily, almost completely filling the combustion chamber above the flameholder. At a value of "y" less than or greater than the critical value, the burning was normal. This effect has been noted by other observers for the unconfined V-flame (Ref. 1).

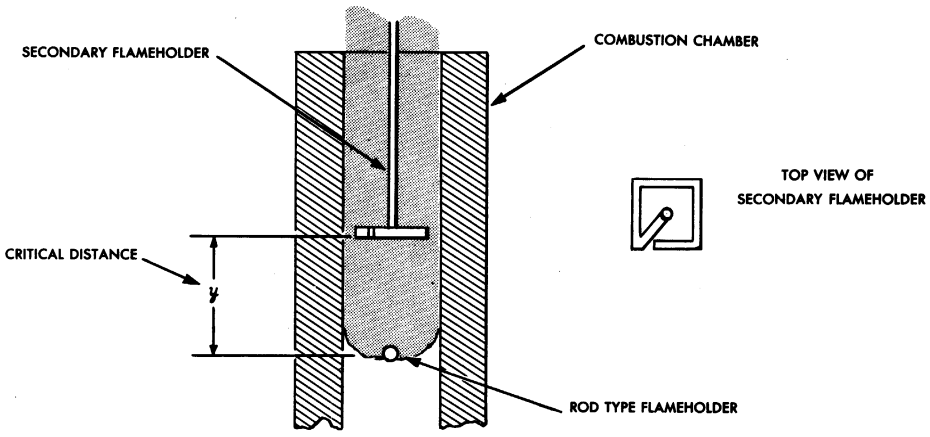

FIG. 21 DIAGRAM OF APPARATUS IN WHICH VIOLENT BURNING IS CAUSED BY A SECONDARY FLAME HOLDER

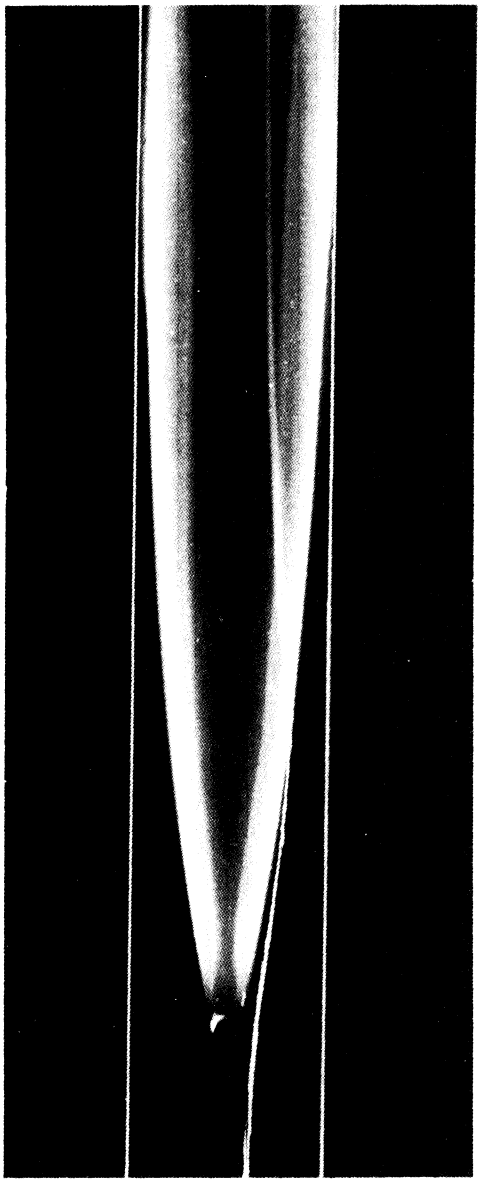

Run No. 13 $V_j = 14.5$ ft./sec.

FIG. 22 STREAMLINE OF $Ti\,Cl_4$ THROUGH FLAME FRONT

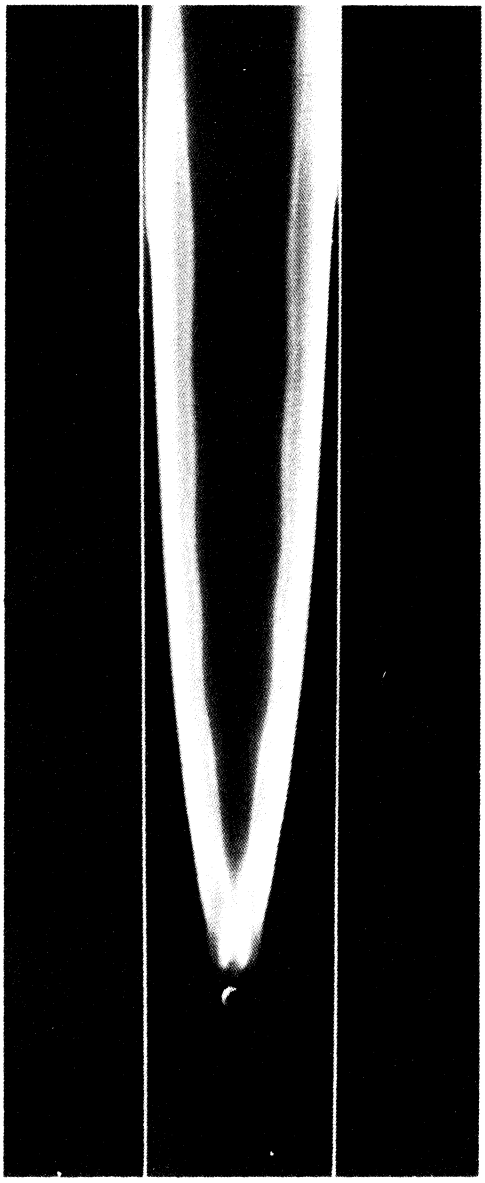

Run No. 34

FIG. 23 STATIONARY WAVE ON INNER FLAME SURFACE

(The streamlines in the unburned gas have been retouched)

4. Under certain conditions a stationary wave was observed on the inner flame surface of the confined V-flame shown in figure 23. There is no obvious reason for this occurring. The inner flame surface is merely the locus of the crests of the wave travelling down the flame front.

CONCLUSIONS

The type of resonant burning described in this report is the type of burning which is obtained for a flame burning in a parallel-walled combustion chamber with all the visible burning taking place within the chamber. The flow process for this type of burning is not steady and hence the resultant flame is considerably different from the Bunsen flame or the unconfined V-flame. Preliminary calculations indicate that flame speeds of the confined and unconfined flames do not differ greatly.

Inasmuch as the ram-jet type burner is essentially a parallel-walled combustion chamber, it seems probable that resonance will always occur in such a burner. For this reason it is felt that an investigation into the cause of resonance and the effect of resonance on flame stability, etc., is necessary for a better understanding of factors governing ram-jet combustion design.

APPENDIX 1

Derivation for the resonant frequency of a column composed of two different gases (Refs. 5, 6, and 7).

1. The one-dimensional wave equation $\frac{\partial^2 y}{\partial t^2} = c^2 \frac{\partial^2 y}{\partial x^2}$ describes the motion of a layer of gas

where y is the displacement of a particle,

where c is the speed of sound, and

where x and t are distance and time.

2. For an open ended combustion chamber the amplitude of the oscillation of the gas will vary as shown below.

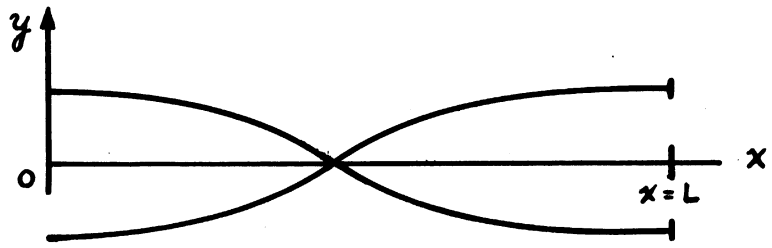

3. Let y vary as cos(2πnt) where n = frequency of oscillation. Then (1) becomes

$$\frac{\partial^2 y}{\partial x^2} + \frac{4\pi^2 n^2 y}{c^2} = 0$$

the solution for which is

$$y = \left(A \cos \frac{2\pi n x}{c} + \beta \sin \frac{2\pi n x}{c}\right) \cos (2\pi n t)$$

4. For an open ended pipe the condensation $\frac{\partial y}{\partial x} = 0$ when x = 0. Hence

$$0 = \left[-A \sin \frac{2\pi n x}{c} \left(\frac{2\pi n}{c}\right) + \beta \frac{2\pi n}{c} \cos \frac{2\pi n x}{c}\right] \cos 2\pi n t$$

resulting in B = 0. Therefore

$$y_1 = A_1 \cos \frac{2\pi nx}{c_1} \cos (2\pi nt)$$

5. For a wave in the second gas:

$$y_2 = [A_2 \cos 2\pi \frac{n(L-x)}{c_2}] \cos (2\pi nt)$$

6. At the intersection of these two waves (flame front) the following conditions must be satisfied:

a. $y_1 = y_2$ The displacements are equal

b. The pressure increment caused by both waves must be equal.

Since $P = P_o + P_o\gamma \frac{\partial y}{\partial x}$ then $\gamma_1 \frac{\partial y_1}{\partial x} = \gamma_2 \frac{\partial y_2}{\partial x}$

7. Condition (6a)

$$A_1 \cos \frac{2\pi nx}{c_1} \cos 2\pi nt = A_2 \cos 2\pi \frac{n(L-x)}{c_2} \cos 2\pi nt$$

or

$$\frac{A_1}{A_2} = \frac{\cos 2\pi n \frac{(L-x)}{c_2}}{\cos 2\pi \frac{nx}{c_1}}$$

8. Condition (6b)

$$-\gamma_1 A_1 \frac{2\pi n}{c_1} \sin \frac{2\pi nx}{c_1} = \gamma_2 A_2 \frac{2\pi n}{c_2} \sin 2\pi \frac{n(L-x)}{c_2}$$

or

$$\frac{A_1}{A_2} = -\frac{c_1\gamma_1}{c_2\gamma_2} \frac{\sin 2\pi \frac{n(L-x)}{c_2}}{\sin 2\pi \frac{nx}{c_1}}$$

9. Equating 7 and 8

$$-c_1\gamma_1 \tan 2\pi \frac{n(L-x)}{c_2} = c_2\gamma_2 \tan \frac{2\pi nx}{c_1}$$

A plot of this function is shown in figure 18.

APPENDIX 2

Calculation of Flame Speeds of the Confined V-flame.

The following calculations are typical of flame speed calculations for the resonant V-flame.

Figure 24 is an enlarged drawing of the shadowgraph taken for run No. 58. The frequency observed was 760 c/s.

1. Calculation of average wave velocity.

As in figure 24 the wave crests will be numbered 0, 1, 2, etc.

Then

$$C = \lambda n = \frac{\text{distance between crests} \times 760}{3.78 \times 12} = \text{distance} \times 16.75$$

$$= \text{wave velocity}$$

Hence

Point	Distance between Wave Crests on Enlargement Inches	C Wave Velocity ft/sec	Distance from 0 to Average Distance between Wave Crests Feet
0	.83	13.9	.0915
1	1.38	23.12	.0335
2	1.87	31.32	.0693
3	2.28	38.19	.1150
4	2.74	43.38	.1688
5	3.17	53.10	.2325
6	3.58	59.96	.3068

A plot of the above values appears in figure 25.

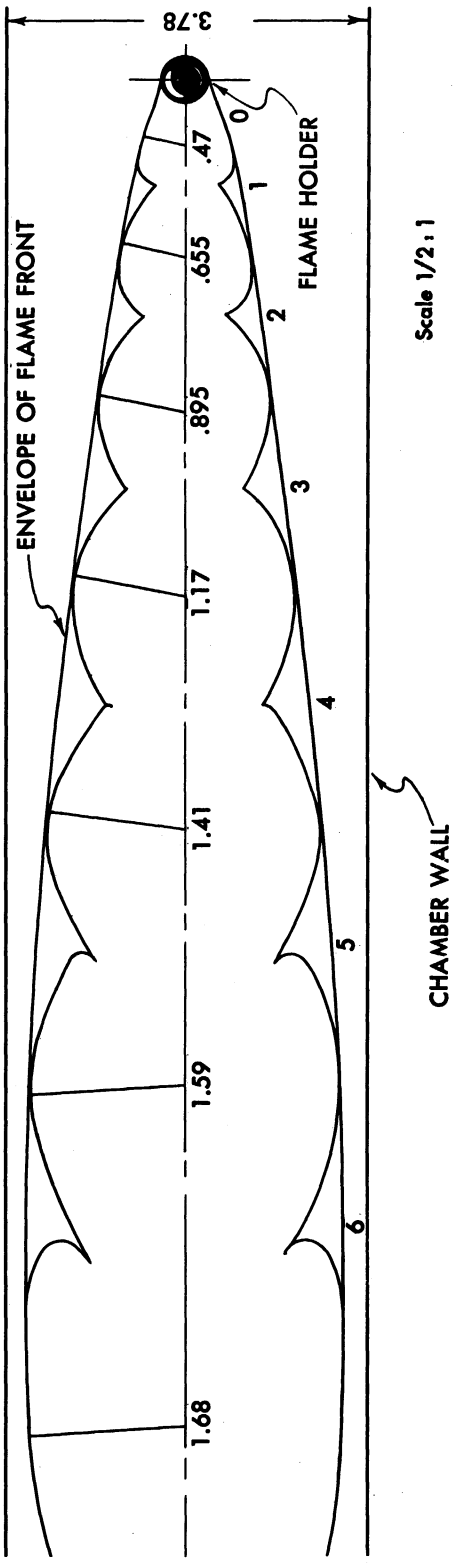

FIG. 24 ENLARGED DRAWING OF CONFINED FLAME

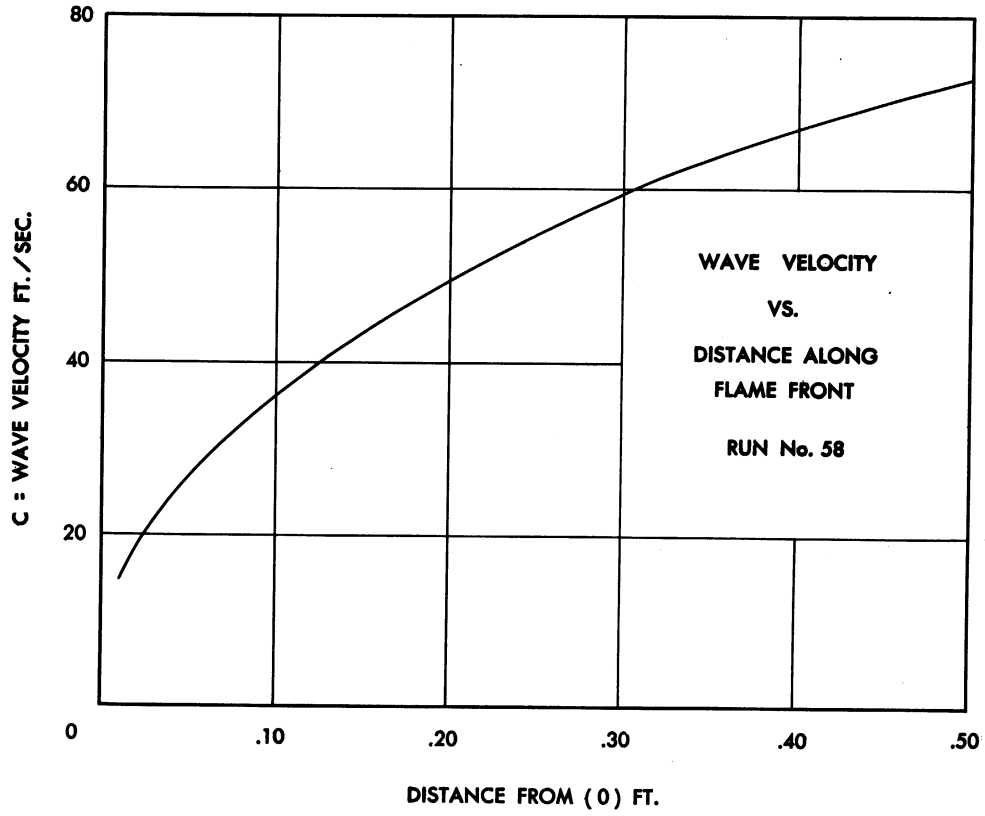

FIG. 25

2. Calculations for flame speeds.

a. Start at some point on the wave front. For a time increment of $\frac{1}{760}$, the distance between this point and a succeeding point is the average velocity multiplied by the fraction $\frac{1}{760}$.

b. At each of the above points a normal is drawn to the flame front.

Point	Distance from (0) Feet	Distance from (0) in Enlargement Inches	r Enlargement Inches	Δr Inches	V_f ft/sec	Average Distance in Feet
0						
	.008	.363	.47	.185 [1]		
1						
	.0312	1.42	.655	.240	.804	.049
2						
	.0661	3.000	.895	.275	.92	.089
3						
	.1112	5.04	1.17	.240	.804	.139
4						
	.1658	7.52	1.41	.180	.60	.198
5						
	.2304	10.45	1.59	.090 [1]		
6						
	.3099	14.06	1.68			
7						

[1] Normals to the flame surface at the points where r is measured are not parallel.

c. These calculations show a variation in flame speed along the flame front. These results are not conclusive, however, due to the inaccuracies in measurement of r. An error of $\pm$ .02" in measuring r from the enlargement causes a maximum variation of flame speed of 3.35 x .04 = .14 l/sec. This error is approximately of the magnitude of the variation found in flame speeds at different positions along the flame front.

Through the use of some other method of obtaining an instantaneous picture of the flame, it would be possible to obtain a better definition of the flame front, hence making it possible to increase the accuracy of the calculations.

APPENDIX 3

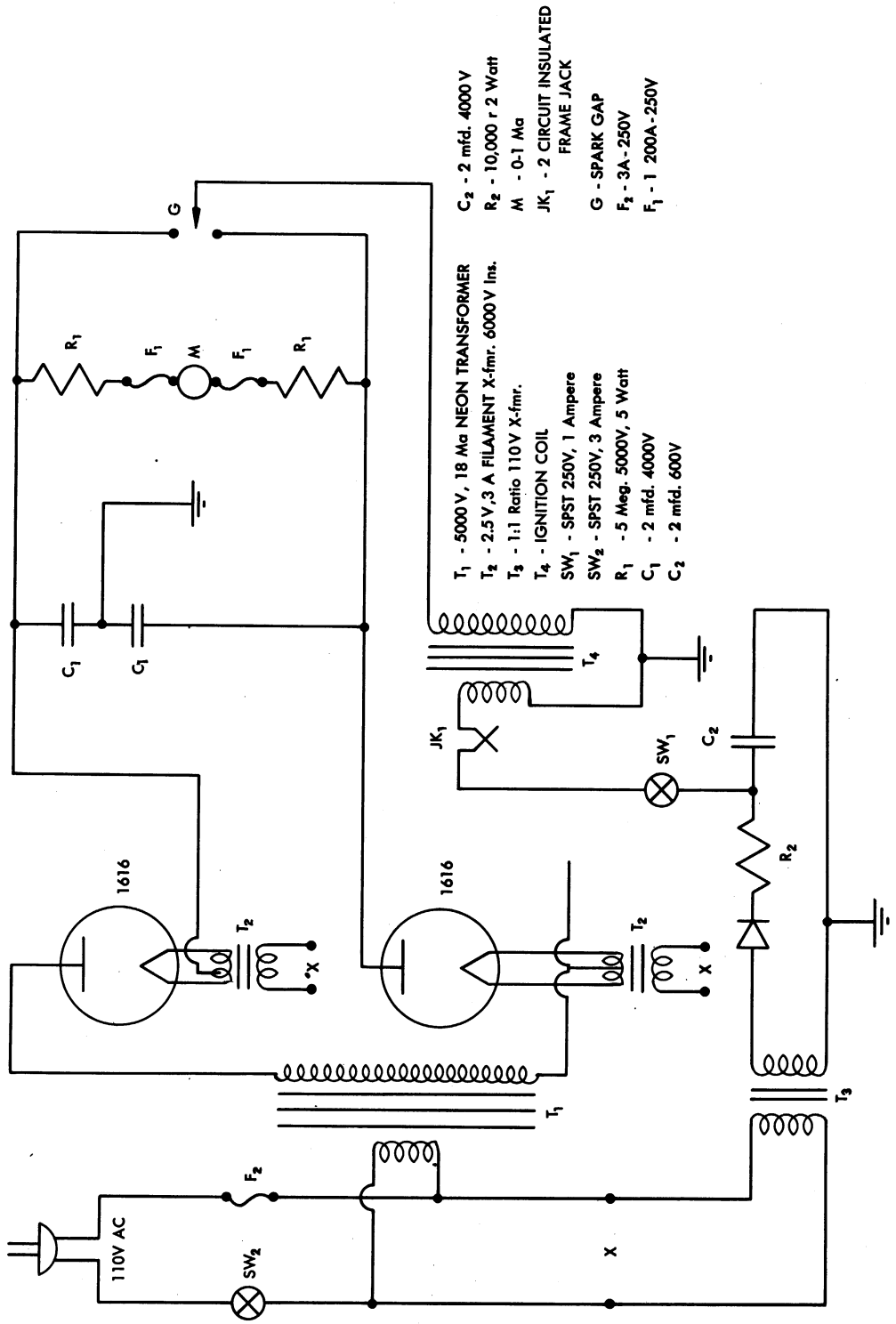

FIG. 26 SCHEMATIC DIAGRAM OF SPARK SOURCE USED FOR SHADOW PHOTOGRAPHY

REFERENCES

1 Progress Report No. 3 (1 August - 1 October 1946), UMR-27, University of Michigan, AAF Contract W33-038 ac 2100.

2 Brown, G. B., Science Progress, Vol. XXVI, No. 101, July, 1931.

3 Coward, Hartwell, and Georgeson, Journal of the Chemical Society, 1937.

4 Scurlock, A. C., Flame Stabilization and Propagation in High Velocity Gas Streams, MIT Meteor Report 19.

5 Lamb, The Dynamical Theory of Sound, Cambridge University Press.

6 Jost, W., Explosion and Combustion Processes in Gases, McGraw-Hill Book Company.

7 Lees, Proceedings of the Physical Society, 41, 204, 1929.

8 Rayleigh, The Theory of Sound, Vol. II, Dover Publications.

9 Morrison, R. B., and R. A. Dunlap, Measurement of Flame Speeds with the V-flame, UMM-21, University of Michigan.

10 White, A. G., Journal of the Chemical Society, 1928.

11 Landau, L., Acta Physicochimica, U.R.S.S., Vol. XIX, No. 1, 1944.

DISTRIBUTION

Distribution of this report is made in accordance with Air Force Letter dated 8 April 1949 MCREXP-3.